Origin of the neutron skin thickness of ^{208}Pb in nuclear mean-field models

M. Centelles,[1,*] X. Roca-Maza,[1,†] X. Viñas,[1,‡] and M. Warda[1,2,§]

[1]*Departament d'Estructura i Constituents de la Matèria and Institut de Ciències del Cosmos, Facultat de Física, Universitat de Barcelona, Diagonal 647, E-08028 Barcelona, Spain*

[2]*Katedra Fizyki Teoretycznej, Uniwersytet Marii Curie–Skłodowskiej, ul. Radziszewskiego 10, PL-20-031 Lublin, Poland*

(Received 14 September 2010; published 19 November 2010)

We study whether the neutron skin thickness Δr_{np} of ^{208}Pb originates from the bulk or from the surface of the nucleon density distributions, according to the mean-field models of nuclear structure, and find that it depends on the stiffness of the nuclear symmetry energy. The bulk contribution to Δr_{np} arises from an extended sharp radius of neutrons, whereas the surface contribution arises from different widths of the neutron and proton surfaces. Nuclear models where the symmetry energy is stiff, as typical of relativistic models, predict a bulk contribution in Δr_{np} of ^{208}Pb about twice as large as the surface contribution. In contrast, models with a soft symmetry energy like common nonrelativistic models predict that Δr_{np} of ^{208}Pb is divided similarly into bulk and surface parts. Indeed, if the symmetry energy is supersoft, the surface contribution becomes dominant. We note that the linear correlation of Δr_{np} of ^{208}Pb with the density derivative of the nuclear symmetry energy arises from the bulk part of Δr_{np}. We also note that most models predict a mixed-type (between halo and skin) neutron distribution for ^{208}Pb. Although the halo-type limit is actually found in the models with a supersoft symmetry energy, the skin-type limit is not supported by any mean-field model. Finally, we compute parity-violating electron scattering in the conditions of the ^{208}Pb parity radius experiment (PREX) and obtain a pocket formula for the parity-violating asymmetry in terms of the parameters that characterize the shape of the ^{208}Pb nucleon densities.

DOI: 10.1103/PhysRevC.82.054314 PACS number(s): 21.10.Gv, 21.60.−n, 21.30.Fe, 25.30.Bf

I. INTRODUCTION

The study of the size and shape of the density distributions of protons and neutrons in nuclei is a classic, yet always contemporary, area of nuclear physics. The proton densities of a host of nuclei are known quite well from the accurate nuclear charge densities measured in experiments involving the electromagnetic interaction [1], like elastic electron scattering. In contrast, the neutron densities have been probed in fewer nuclei and are generally much less certain.

The neutron distribution of ^{208}Pb, and its rms radius in particular, is nowadays attracting significant interest in both experiment and theory. Indeed, the neutron skin thickness, that is, the neutron-proton rms radius difference

$$\Delta r_{np} = \langle r^2 \rangle_n^{1/2} - \langle r^2 \rangle_p^{1/2}, \tag{1}$$

of this nucleus has close ties with the density-dependent nuclear symmetry energy and with the equation of state of neutron-rich matter. In nuclear models, Δr_{np} of ^{208}Pb displays nearly linear correlations with the slope of the equation of state of neutron matter [2–4], with the density derivative L of the symmetry energy [5–11], and with the surface-symmetry energy of the finite nucleus [9]. At first sight, it may seem intriguing that a property of the mean position of the surface of the nucleon densities (Δr_{np}) is correlated with a purely bulk property of infinite nuclear matter (L). However, we have to keep in mind that Δr_{np} depends on the surface-symmetry energy. This quantity reduces the bulk-symmetry energy due to the finite size of the nucleus. Assuming a local density approximation, we can correlate the surface-symmetry energy with the density slope L, which determines the departure of the symmetry energy from the bulk value. The correlation of Δr_{np} with L then follows. Actually, these correlations can be derived almost analytically starting from the droplet model (DM) of Myers and Świątecki [12,13], as we showed in Refs. [9,10]. By reason of its close connections with the nuclear symmetry energy, knowing accurately Δr_{np} of ^{208}Pb can have important implications in diverse problems of nuclear structure and of heavy-ion reactions, in studies of atomic parity violation, as well as in the description of neutron stars and in other areas of nuclear astrophysics (see, e.g., Refs. [14–28]). Since the charge radius of ^{208}Pb has been measured with extreme accuracy ($r_{\rm ch} = 5.5013(7)$ fm [1]), the neutron rms radius of ^{208}Pb is the principal unknown piece of the puzzle.

The lead parity radius experiment (PREX) [29] is a challenging experimental effort that aims to determine $\langle r^2 \rangle_n^{1/2}$ of ^{208}Pb almost model independently and to 1% accuracy by parity-violating electron scattering [29,30]. This purely electroweak experiment was run at the Jefferson Lab very recently, although results are not yet available. The parity-violating electron scattering is useful to measure neutron densities because, in the low-momentum transfer regime, the Z^0 boson couples mainly to neutrons. For protons, this coupling is highly suppressed because of the value of the Weinberg angle. Therefore, from parity-violating electron scattering one can obtain the weak charge form factor and the closely related neutron form factor. From these data, the neutron rms radius can in principle be deduced [30]. This

*mariocentelles@ub.edu
†roca@ecm.ub.es
‡xavier@ecm.ub.es
§warda@kft.umcs.lublin.pl

way of proceeding is similar to how the charge density is obtained from unpolarized electron scattering data [30]. The electroweak experiments are free of the complexities of the hadronic interactions and the reaction mechanism does not have to be modeled. Thus, the analysis of the data can be both clean and model independent. There may be a certain model dependence, in the end, in having to use some neutron density shape to extract the neutron rms radius from the parity-violating asymmetry measured at a finite momentum transfer.

To date, the existing constraints on neutron radii, skins, and neutron distributions of nuclei have mostly used strongly interacting hadronic probes. Unfortunately, the measurements of neutron distributions with hadronic probes are bound to have some model dependence because of the uncertainties associated with the strong force. Among the more frequent experimental techniques, we may quote nucleon elastic scattering [31,32], the inelastic excitation of the giant dipole and spin-dipole resonances [33,34], and experiments in exotic atoms [35–38]. Recent studies indicate that the pygmy dipole resonance may be another helpful tool to constrain neutron skins [21,27].

The extraction of neutron radii and neutron skins from the experiment is intertwined with the dependence of these quantities on the shape of the neutron distribution [35–39]. The data typically do not indicate unambiguously, by themselves, if the difference between the peripheral neutron and proton densities that gives rise to the neutron skin is caused by an extended bulk radius of the neutron density, by a modification of the width of the surface, or by some combination of both effects. In the present work, we look for theoretical indications of this problem and study whether the origin of the neutron skin thickness of ^{208}Pb comes from the bulk or from the surface of the nucleon densities according to the mean-field models of nuclear structure. The answer turns out to be connected to the density dependence of the nuclear symmetry energy in the theory.

We described in Ref. [40] a procedure to discern bulk and surface contributions in the neutron skin thickness of nuclei. It can be applied to both theoretical and experimental nucleon densities because it only requires knowledge of the equivalent sharp radius and surface width of these densities, which one can obtain by fitting the actual densities with two-parameter Fermi (2pF) distributions. The 2pF shape is commonly used to characterize nuclear densities and nuclear potentials in both theoretical and experimental analyses. The doubly magic number of protons and neutrons in ^{208}Pb ensures that deformations do not influence the results and spherical density distributions describe the nuclear surface very well. We perform our calculations with several representative effective nuclear forces, namely, nonrelativistic interactions of the Skyrme and Gogny type and relativistic mean-field (RMF) interactions. The free parameters and coupling constants of these nuclear interactions have usually been adjusted to describe data that are well known empirically, such as binding energies, charge radii, single-particle properties, and several features of the nuclear equation of state. However, the same interactions predict widely different results for the size of neutron skin of ^{208}Pb and, as we will see, for its bulk or surface nature. We also study the halo or skin character [35–39] of the nucleon densities of ^{208}Pb in mean-field models. Finally, we perform calculations of parity-violating electron scattering on ^{208}Pb. We show that, if 2pF nucleon densities are assumed, the parity-violating asymmetry as predicted by mean-field models can be approximated by a simple and analytical expression in terms of the central radius and surface width of the neutron and proton density profiles. This suggests that an experiment such as PREX could allow some information to be obtained about the neutron density profile of the ^{208}Pb nucleus in addition to its neutron rms radius.

The rest of the article proceeds as follows. In Sec. II, we summarize the formalism to decompose the neutron skin thickness into bulk and surface components. The results obtained in the nuclear mean-field models are presented and discussed in Sec. III. A summary and the conclusions are given in Sec. IV.

II. FORMALISM

The analysis of bulk and surface contributions to the neutron skin thickness of a nucleus requires proper definitions of these quantities based on nuclear density distributions. We presented such a study in Ref. [40], and we summarize only its basic points here.

One can characterize the size of a nuclear density distribution $\rho(r)$ through several definitions of radii, and each definition may be more useful for a specific purpose (see Ref. [41] for a thorough review). Among the most common radii, we have the *central radius* C,

$$C = \frac{1}{\rho(0)} \int_0^\infty \rho(r) dr; \tag{2}$$

the *equivalent sharp radius* R,

$$\frac{4}{3}\pi R^3 \rho(\text{bulk}) = 4\pi \int_0^\infty \rho(r) r^2 dr, \tag{3}$$

that is, the radius of a uniform sharp distribution whose density equals the bulk value of the actual density and has the same number of particles; and the *equivalent rms radius* Q,

$$\tfrac{3}{5} Q^2 = \langle r^2 \rangle, \tag{4}$$

which describes a uniform sharp distribution with the same rms radius as the given density. These three radii are related by expansion formulas [41]:

$$Q = R\left(1 + \frac{5}{2}\frac{b^2}{R^2} + \cdots\right), \quad C = R\left(1 - \frac{b^2}{R^2} + \cdots\right). \tag{5}$$

Here, b is the *surface width* of the density profile:

$$b^2 = -\frac{1}{\rho(0)} \int_0^\infty (r - C)^2 \frac{d\rho(r)}{dr} dr, \tag{6}$$

which provides a measure of the extent of the surface of the density. Relations (5) usually converge quickly because b/R is small in nuclei, especially in heavy-mass systems. Nuclear density distributions have oscillations in the inner bulk region and a meaningful average is needed to determine the density values $\rho(0)$ and $\rho(\text{bulk})$ appearing in the above equations. This

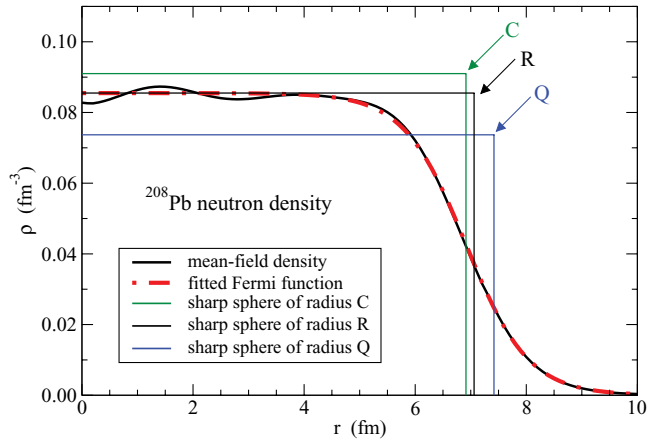

FIG. 1. (Color online) Comparison of sharp density profiles having radii C, R, and Q with the mean-field and 2pF density distributions for the neutron density of ^{208}Pb. The RMF interaction NL3 has been used in the mean-field calculation.

can be achieved by matching the original density with a 2pF distribution:

$$\rho(r) = \frac{\rho_0}{1 + \exp\left[(r - C)/a\right]}. \tag{7}$$

In 2pF functions the bulk density value corresponds very closely to the central density, and the latter coincides to high accuracy with the ρ_0 parameter if $\exp(-C/a)$ is negligible. The surface width b and the diffuseness parameter a of a 2pF function are related by $b = (\pi/\sqrt{3})a$.

As discussed in Ref. [41], the equivalent sharp radius R is the quantity of basic geometric importance of the C, Q, and R radii. This is because a sharp distribution of radius R has the same volume integral as the density of the finite nucleus and differs from it only in the surface region. We illustrate this fact in Fig. 1 using as an example the neutron density of ^{208}Pb of a mean-field calculation. We can see that the mean-field density is clearly overestimated in the whole nuclear interior by a sharp sphere of radius C. The equivalent rms radius Q fails also, by underestimating it. Only the equivalent sharp radius R is able to reproduce properly the bulk part of the original density profile of the nucleus. Therefore, R appears as the suitable radius to describe the size of the bulk of the nucleus.

As the neutron skin thickness (1) is defined through rms radii, it can be expressed with Q:

$$\Delta r_{np} = \sqrt{\frac{3}{5}}(Q_n - Q_p). \tag{8}$$

Recalling from Eqs. (5) that $Q \simeq R + \frac{5}{2}(b^2/R)$, we have a natural distinction in Δr_{np} between bulk ($\propto R_n - R_p$) and surface contributions. That is to say,

$$\Delta r_{np} = \Delta r_{np}^{\rm bulk} + \Delta r_{np}^{\rm surf}, \tag{9}$$

with

$$\Delta r_{np}^{\rm bulk} = \sqrt{\frac{3}{5}}(R_n - R_p) \tag{10}$$

independent of surface properties, and

$$\Delta r_{np}^{\rm surf} = \sqrt{\frac{3}{5}}\frac{5}{2}\left(\frac{b_n^2}{R_n} - \frac{b_p^2}{R_p}\right) \tag{11}$$

of surface origin. The nucleus may develop a neutron skin by separation of the bulk radii R of neutrons and protons or by modification of the width b of the surfaces of the neutron and proton densities. In the general case, both effects are expected to contribute. We note that Eq. (11) coincides with the expression of the surface width contribution to the neutron skin thickness provided by the DM of Myers and Świątecki [12,13] if we set $R_n = R_p = r_0 A^{1/3}$ in Eq. (11).

The next-order correction to Eq. (11) can be easily evaluated for 2pF distributions (cf. Ref. [41] for the higher-order corrections to expansions (5)) and gives

$$\Delta r_{np}^{\rm surf,corr} = -\sqrt{\frac{3}{5}}\frac{5}{2}\frac{21}{20}\left(\frac{b_n^4}{R_n^3} - \frac{b_p^4}{R_p^3}\right). \tag{12}$$

This quantity is usually very small—indeed, we neglected it in Ref. [40]. In the case of ^{208}Pb, we found in all calculations with mean-field models that it is between -0.0025 and -0.004 fm, and thus can be obviated for most purposes. But because in the present work we deal with some detailed comparisons among the models, we have included Eq. (12) in the numerical values shown for the surface contribution $\Delta r_{np}^{\rm surf}$ in the later sections.

It is to be mentioned that there is no universal method to perform the parametrization of the neutron and proton densities with 2pF functions. A popular prescription is to use a χ^2 minimization of the differences between the density to be reproduced and the 2pF profile, or of the differences between their logarithms. These methods may somewhat depend on conditions given during minimization (number of mesh points, limits, etc.). As in Ref. [40], we preferred to extract the parameters of the 2pF profiles by imposing that they reproduce the same quadratic $\langle r^2\rangle$ and quartic $\langle r^4\rangle$ moments of the self-consistent mean-field densities, and the same number of nucleons. These conditions allow us to determine in a unique way the equivalent 2pF densities and to pay attention to a good reproduction of the surface region of the original density because the local distributions of the quantities $r^2\rho(r)$ and $r^4\rho(r)$ are peaked at the peripheral region of the nucleus. An example of this type of fit is displayed in Fig. 1 by the dash-dotted line. It can be seen that the equivalent 2pF distribution nicely averages the quantal oscillations at the interior and reproduces accurately the behavior of the mean-field density at the surface.

III. RESULTS

A. Survey of model predictions and of data for Δr_{np} of ^{208}Pb

We calculated our results with nonrelativistic models of Skyrme type (SGII, Ska, SkM*, Sk-T4, Sk-T6, Sk-Rs, SkMP, SkSM*, MSk7, SLy4, HFB-8, and HFB-17) and of Gogny type (D1S, D1N), as well as with several relativistic models (NL1, NL-Z, NL-SH NL-RA1, NL3, TM1, NLC, G2, FSUGold, DD-ME2, and NL3*). The original references to the different interactions can be found in Refs. [23,42] for the Skyrme models, Ref. [43] for the Gogny models, and Refs. [44–48]

(and Ref. [19] in Ref. [44]) for the RMF models. It may be mentioned that the recent force HFB-17 [42] achieves the lowest rms deviation with respect to experimental nuclear masses found to date in a mean-field approach.

As is well known, nonrelativistic and relativistic models differ in the stiffness of the symmetry energy. Note that by soft or stiff symmetry energy we mean that the symmetry energy increases slowly or rapidly as a function of the nuclear density around the saturation point. Of course, the soft or stiff character can depend on the explored density region; for example, it is possible that a symmetry energy that is soft at nuclear densities becomes stiff at much higher densities [49], or that a model with a stiff symmetry energy at normal density has a smaller symmetry energy at low densities [50]. The density dependence of the nuclear symmetry energy $c_{\rm sym}(\rho)$ around saturation is frequently parametrized through the slope L of $c_{\rm sym}(\rho)$ at the saturation density:

$$L = 3\rho_0 \frac{\partial c_{\rm sym}(\rho)}{\partial \rho}\bigg|_{\rho_0}. \tag{13}$$

The pressure of pure neutron matter is directly proportional to L [51] and thus the L value has important implications for both neutron-rich nuclei and neutron stars. The symmetry energy of the Skyrme and Gogny forces analyzed in this work displays, as usual in the nonrelativistic models, from very soft to moderately stiff density dependence at nuclear densities (see Table I for the L parameter of the models). However, the majority of the relativistic parameter sets have a stiff or very stiff symmetry energy around saturation. The exceptions to the last statement in our case are the covariant parameter sets FSUGold and DD-ME2 that have a milder symmetry energy than the typical RMF models. FSUGold achieves this through an isoscalar-isovector nonlinear meson coupling [46] and DD-ME2 from having density-dependent meson-exchange couplings [47].

In Table I we display the neutron skin thickness of ^{208}Pb obtained from the self-consistent densities of the various interactions (denoted as $\Delta r_{np}^{\rm sc}$). It is evident that the nuclear mean-field models predict a large window of values for this quantity. The nonrelativistic models with softer symmetry energies point toward a range of about 0.1–0.17 fm. Most of the relativistic models, having a stiff symmetry energy, point toward larger neutron skins of 0.25–0.3 fm. In between, the relativistic models DD-ME2 and FSUGold predict a result close to 0.2 fm, and the Skyrme interactions that have relatively stiffer symmetry energies fill in the range between 0.2 and 0.25 fm.

Before proceeding, we would like to briefly survey some of the recent results deduced for Δr_{np} in ^{208}Pb from experiment. For example, the recent analysis in Ref. [52] of the data measured in the antiprotonic ^{208}Pb atom [35,36] gives $\Delta r_{np} = 0.16 \pm (0.02)_{\rm stat} \pm (0.04)_{\rm syst}$ fm, including statistical and systematic errors. Another recent study [53] of the antiprotonic data for the same nucleus leads to $\Delta r_{np} = 0.20 \pm (0.04)_{\rm exp} \pm (0.05)_{\rm theor}$ fm, where the theoretical error is suggested from comparison of the models with the experimental charge density. These determinations are in consonance with the *average* value of the hadron scattering data for the neutron skin thickness of ^{208}Pb, namely, $\Delta r_{np} \sim 0.165 \pm 0.025$ fm (taken from the compilation of hadron scattering data in Fig. 3 of Ref. [36]). We may also mention that the constraints on the nuclear symmetry energy derived from isospin diffusion in heavy-ion collisions of neutron-rich nuclei suggest $\Delta r_{np} = 0.22 \pm 0.04$ fm in ^{208}Pb [54]. Following Ref. [55], the same type of constraints exclude Δr_{np} values in ^{208}Pb less than 0.15 fm. A recent prediction based on measurements of the pygmy dipole resonance in ^{68}Ni and ^{132}Sn gives $\Delta r_{np} = 0.194 \pm 0.024$ fm in ^{208}Pb [27]. Finally, we quote the new value $\Delta r_{np} = 0.211^{+0.054}_{-0.063}$ fm determined in [56] from proton elastic scattering. Thus, in view of the empirical information for the central value of Δr_{np} and in view of the $\Delta r_{np}^{\rm sc}$ values predicted by the theoretical models in Table I, it may be said that those interactions with a soft (but not very soft) symmetry energy, for example, HFB-17, SLy4, SkM*, DD-ME2, or FSUGold, agree better with the determinations from experiment. Nevertheless, the uncertainties in the available information for Δr_{np} are rather large and one cannot rule out the predictions by other interactions. If PREX [29,30] achieves the purported goal of accurately measuring the neutron rms radius of ^{208}Pb, it will allow us to pin down more strictly the constraints on the neutron skin thickness of the mean-field models.

TABLE I. Neutron skin thickness in ^{208}Pb calculated with the self-consistent densities of several nuclear mean-field models ($\Delta r_{np}^{\rm sc}$) and its partition into bulk and surface contributions defined in Sec. II, as well as the relative weight of these bulk and surface parts.[a]

Model	$\Delta r_{np}^{\rm sc}$ (fm)	$\Delta r_{np}^{\rm bulk}$ (fm)	$\Delta r_{np}^{\rm surf}$ (fm)	Bulk (%)	Surface (%)	L (MeV)
HFB-8	0.115	0.031	0.084	27	73	14.8
MSk7	0.116	0.030	0.086	26	74	9.4
D1S	0.135	0.062	0.073	46	54	22.4
SGII	0.136	0.065	0.071	48	52	37.6
D1N	0.142	0.070	0.072	49	51	31.9
Sk-T6	0.151	0.067	0.084	44	56	30.9
HFB-17	0.151	0.067	0.084	44	56	36.3
SLy4	0.161	0.086	0.075	53	47	46.0
SkM*	0.170	0.093	0.077	55	45	45.8
DD-ME2[b]	0.193	0.098	0.095	51	49	51.3
SkSM*	0.197	0.116	0.082	58	42	65.5
SkMP	0.197	0.123	0.074	62	38	70.3
FSUGold[b]	0.207	0.105	0.102	51	49	60.5
Ska	0.211	0.140	0.071	66	34	74.6
Sk-Rs	0.215	0.146	0.069	68	32	85.7
Sk-T4	0.248	0.163	0.085	66	34	94.1
G2[b]	0.257	0.171	0.086	66	34	100.7
NLC[b]	0.263	0.174	0.089	66	34	108.0
NL-SH[b]	0.266	0.169	0.097	64	36	113.6
TM1[b]	0.271	0.172	0.098	64	36	110.8
NL-RA1[b]	0.274	0.179	0.095	65	35	115.4
NL3[b]	0.280	0.185	0.095	66	34	118.5
NL3*[b]	0.288	0.191	0.097	66	34	122.6
NL-Z[b]	0.307	0.209	0.098	68	32	133.3
NL1[b]	0.321	0.216	0.105	67	33	140.1

[a]The models have been set out according to increasing $\Delta r_{np}^{\rm sc}$. The density slope L of the symmetry energy of the models is also listed.
[b]Denotes relativistic models.

B. Bulk and surface contributions to Δr_{np} of ^{208}Pb in nuclear models and the symmetry energy

We next discuss the results for the division of the neutron skin thickness of ^{208}Pb into bulk ($\Delta r_{np}^{\rm bulk}$) and surface ($\Delta r_{np}^{\rm surf}$) contributions in the nuclear mean-field models, following Sec. II. We display this information in Table I. It may be noticed that the value of $\Delta r_{np}^{\rm bulk}$ plus $\Delta r_{np}^{\rm surf}$ [quantities obtained from Eqs. (10)–(12)] agrees excellently with $\Delta r_{np}^{\rm sc}$ (neutron skin thickness obtained from the self-consistent densities). One finds that the bulk contribution $\Delta r_{np}^{\rm bulk}$ to the neutron skin of ^{208}Pb varies in a window from about 0.03 to 0.22 fm. The surface contribution $\Delta r_{np}^{\rm surf}$ comprises approximately between 0.07 and 0.085 fm in the nonrelativistic forces, and between 0.085 and 0.105 fm in the relativistic ones. Thus, whereas the bulk contribution to the neutron skin thickness of ^{208}Pb changes largely among the different mean-field models, the surface contribution remains confined to a narrower band of values.

Table I shows that the size of the neutron skin thickness of ^{208}Pb is divided into bulk and surface contributions in almost equal parts in the nuclear interactions that have soft symmetry energies (say, $L \sim 20$–60). This is the case of multiple nonrelativistic interactions and of the covariant DD-ME2 and FSUGold parameter sets. When the symmetry energy becomes softer, the bulk part tends to be smaller. Indeed, we see that in the models that have a very soft symmetry energy ($L \lesssim 20$), which we may call "supersoft" [57], the surface contribution takes over and it is responsible for the largest part (∼75%) of Δr_{np} of ^{208}Pb. At variance with this situation, in the models with stiffer symmetry energies ($L \gtrsim 75$), about two thirds of Δr_{np} of ^{208}Pb come from the bulk contribution, as seen in the Skyrme forces of stiffer symmetry energy and in all of the relativistic forces that have a conventional isovector channel (G2, TM1, NL3, etc.). We therefore note that, in a heavy neutron-rich nucleus with a sizable neutron skin such as ^{208}Pb, the nuclear interactions with a soft symmetry energy predict that the contribution to Δr_{np} produced by differing widths of the surfaces of the neutron and proton densities ($b_n \neq b_p$) is similar to, or even larger than, the effect from differing extensions of the bulk of the nucleon densities ($R_n \neq R_p$). However, the nuclear interactions with a stiff symmetry energy favor a dominant bulk nature of the neutron skin of ^{208}Pb, and then the largest part of Δr_{np} is caused by $R_n \neq R_p$. We collect in Table II the found equivalent sharp radii R_n and R_p and surface widths b_n and b_p of the densities of ^{208}Pb in the present mean-field models.

As we have had the opportunity to see, the neutron skin thickness of a heavy nucleus is strongly influenced by the density derivative L of the symmetry energy. Indeed, one easily suspects from Table I that Δr_{np} of ^{208}Pb is almost linearly correlated with L in the nuclear mean-field models, which Fig. 2 confirms for the present interactions. The correlation of the neutron skin thickness of ^{208}Pb with L has been amply discussed in the literature [5–11], because it implies that an accurate measurement of the former observable could allow the density dependence of the nuclear symmetry energy to be tightly constrained. In particular, we studied the aforementioned correlation in Ref. [9], where it is shown that

TABLE II. Equivalent sharp radius and surface width of the 2pF neutron and proton density distributions of ^{208}Pb in mean-field models (units are fm).

Model	R_n	R_p	b_n	b_p
HFB-8	6.822	6.782	0.991	0.819
MSk7	6.847	6.808	0.980	0.801
D1S	6.830	6.751	0.994	0.846
SGII	6.890	6.806	0.971	0.821
D1N	6.845	6.755	0.979	0.828
Sk-T6	6.862	6.775	0.994	0.820
HFB-17	6.883	6.797	0.996	0.821
SLy4	6.902	6.790	1.007	0.852
SkM*	6.907	6.786	1.007	0.847
DD-ME2	6.926	6.800	1.026	0.829
SkSM*	6.955	6.805	0.970	0.790
SkMP	6.943	6.784	0.997	0.839
FSUGold	6.971	6.836	1.024	0.808
Ska	6.970	6.789	0.998	0.844
Sk-Rs	6.950	6.762	0.962	0.806
Sk-T4	6.991	6.780	1.008	0.823
G2	7.037	6.817	1.012	0.824
NLC	7.087	6.863	1.016	0.820
NL-SH	7.039	6.821	0.989	0.772
TM1	7.085	6.862	1.005	0.787
NL-RA1	7.065	6.834	1.008	0.797
NL3	7.060	6.821	1.017	0.807
NL3*	7.052	6.806	1.026	0.814
NL-Z	7.134	6.865	1.058	0.847
NL1	7.100	6.822	1.065	0.840

the expression of the neutron skin thickness in the DM of Myers and Świątecki [12,13] can be recast to leading order in terms of the L parameter. To do that, we use the fact that in all mean-field models the symmetry energy coefficient computed at $\rho \approx 0.10$ fm^{-3} is approximately equal to the DM symmetry energy coefficient in ^{208}Pb, which includes bulk- and surface-symmetry contributions [9]. In the standard DM, where the surface widths of the neutron and proton densities

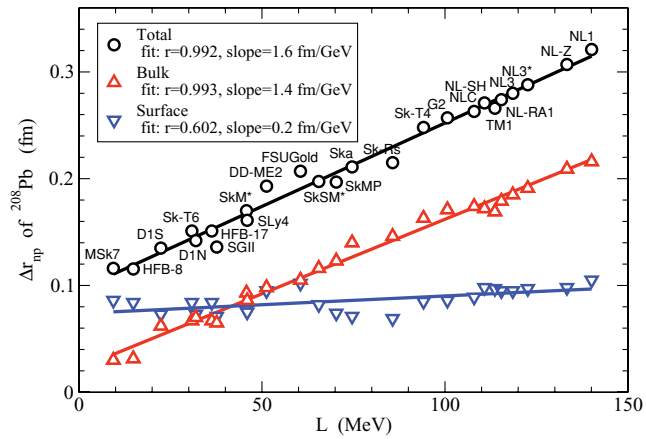

FIG. 2. (Color online) Correlation of the neutron skin thickness of ^{208}Pb and of its bulk and surface parts with the density derivative L of the nuclear symmetry energy.

are taken to be the same [12,13], the neutron skin thickness is governed by the ratio between the bulk-symmetry energy at saturation, $J \equiv c_{\rm sym}(\rho_0)$, and the surface stiffness coefficient Q of the DM [9,10] [the latter is not to be confused with the equivalent rms radius Q of Eq. (4)]. The DM coefficient Q measures the resistance of the nucleus against the separation of the neutron and proton surfaces to form a neutron skin. We have shown [9,10] in mean-field models that the DM formula for the neutron skin thickness, in the case where one assumes $b_n = b_p$, undershoots the corresponding values computed by the semiclassical extended Thomas-Fermi method in finite nuclei and, therefore, a nonvanishing surface contribution is needed to describe more accurately the mean-field results. However, this surface contribution has a more involved dependence on the parameters of the interaction and does not show a definite correlation with the J/Q ratio (see Fig. 4 of Ref. [10]).

Now, we wondered to which degree the correlation with L of the neutron skin thickness of ^{208}Pb holds in its bulk and surface parts extracted from actual mean-field densities. From our discussion of the indications provided by the DM, we can expect this correlation to be strong in the bulk part and weak in the surface part. Indeed, the plots of $\Delta r_{np}^{\rm bulk}$ and $\Delta r_{np}^{\rm surf}$ against L in Fig. 2 show that the bulk part displays the same high correlation with L as the total neutron skin (the linear correlation factor is 0.99 in both cases), whereas the surface part exhibits a mostly flat trend with L. The linear fits in Fig. 2 of the neutron skin thickness of ^{208}Pb and of its bulk part also have quite similar slopes. One thus concludes that the linear correlation of Δr_{np} of ^{208}Pb with the density content of the nuclear symmetry energy arises mainly from the bulk part of Δr_{np}. In other words, the correlation arises from the change induced by the density dependence of the symmetry energy in the equivalent sharp radii of the nucleon density distributions of ^{208}Pb rather than from the change of the width of the surface of the nucleon densities.

The value of about 0.1 fm that the surface contribution to Δr_{np} takes in ^{208}Pb can be understood as follows, starting from Eq. (11). Taking into account that in 2pF distributions fitted to mean-field densities $R_n \sim R_p \sim 1.16A^{1/3}$ fm and $b_n + b_p \sim 1.8$ fm (see Table II), Eq. (11) can be approximated as

$$\Delta r_{np}^{\rm surf} \sim 3A^{-1/3}(b_n - b_p). \tag{14}$$

Given that $b_n - b_p \sim 0.2$ fm for ^{208}Pb on the average in mean-field models (see Table II), one finds $\Delta r_{np}^{\rm surf} \sim 0.1$ fm, rather independently of the model used to compute it. It is interesting why the range of variation of b_n with respect to b_p is not larger in nuclear models, in view of the fact that $R_n - R_p$ can take more different values. As discussed in Ref. [30], this constraint is imposed on the models most likely by the mass fits. For example, a model having nucleon densities with very small or very large surface widths (i.e., very sharp or very extended surfaces) would provoke a large change in the surface energy of the nucleus, but that hardly would be successful to reproduce the known nuclear masses.

C. Discussion of the shape of the neutron density profiles

The use of 2pF functions to represent the nuclear densities by approximate distributions is also quite common in the experimental investigations. The parameters of the proton 2pF distribution can be assumed known in experiments, by unfolding from the accurately measured charge density [40]. However, the shape of the neutron density is more uncertain, and, even if the neutron rms radius is determined, it can correspond to different shapes of the neutron density. Actually, the shape of the neutron density is a significant question in the extraction of nuclear information from experiments in exotic atoms [35–38] and from parity-violating electron scattering [39]. To handle the possible differences in the shape of the neutron density when analyzing the experimental data, the "halo" and "skin" forms are frequently used [35–39]. In the halo-type distribution, the nucleon 2pF shapes have $C_n = C_p$ and $a_n > a_p$, whereas in the skin-type distribution they have $a_n = a_p$ and $C_n > C_p$. To complete our study, we believe the predictions of the theoretical models for the parameters of the 2pF shapes in ^{208}Pb are worth discussion.

TABLE III. Central radius and surface diffuseness of the 2pF neutron and proton density distributions of ^{208}Pb in mean-field models (units are fm).

Model	C_n	C_p	a_n	a_p	$C_n - C_p$	$a_n - a_p$
HFB-8	6.679	6.683	0.546	0.451	−0.004	0.095
MSk7	6.707	6.714	0.540	0.442	−0.007	0.099
D1S	6.687	6.649	0.546	0.464	0.038	0.082
SGII	6.753	6.707	0.536	0.453	0.046	0.083
D1N	6.705	6.657	0.537	0.453	0.048	0.084
Sk-T6	6.718	6.676	0.548	0.452	0.042	0.096
HFB-17	6.739	6.697	0.549	0.453	0.042	0.096
SLy4	6.755	6.683	0.555	0.470	0.072	0.085
SkM*	6.760	6.681	0.555	0.467	0.079	0.088
DD-ME2	6.774	6.699	0.566	0.457	0.075	0.109
SkSM*	6.819	6.713	0.535	0.436	0.106	0.099
SkMP	6.799	6.680	0.550	0.463	0.119	0.087
FSUGold	6.821	6.740	0.564	0.446	0.081	0.118
Ska	6.827	6.684	0.550	0.465	0.143	0.085
Sk-Rs	6.817	6.665	0.530	0.444	0.152	0.086
Sk-T4	6.846	6.681	0.555	0.453	0.165	0.102
G2	6.891	6.717	0.558	0.454	0.174	0.104
NLC	6.941	6.765	0.560	0.452	0.176	0.108
NL-SH	6.900	6.733	0.546	0.426	0.167	0.120
TM1	6.942	6.772	0.554	0.434	0.170	0.120
NL-RA1	6.921	6.741	0.556	0.440	0.180	0.116
NL3	6.914	6.726	0.560	0.445	0.188	0.115
NL3*	6.903	6.709	0.566	0.449	0.194	0.117
NL-Z	6.977	6.761	0.584	0.467	0.216	0.117
NL1	6.940	6.718	0.587	0.463	0.222	0.124

We compile in Table III the central radii C_n and C_p and the diffuseness parameters a_n and a_p of the 2pF nucleon density profiles of ^{208}Pb obtained from the mean-field models of Table I. We see that C_n of neutrons spans a range of approximately 6.7 to 6.85 fm in the nonrelativistic interactions and that it is of approximately 6.8 to 7 fm in the relativistic parameter sets. In the case of the proton density distribution, the value of C_p is smallest (∼6.65 fm) in the two Gogny forces, it is about 6.67–6.71 fm in the Skyrme forces, and it is in the range 6.7–6.77 fm in the RMF models. Then, we

note that not only C_n of neutrons but also C_p of protons is generally smaller in the nonrelativistic forces than in the relativistic forces. The total spread in C_p among the models (about 0.12 fm) is, however, less than half the spread found in C_n (about 0.3 fm). Indeed, the accurately known charge radius of ^{208}Pb is an observable that usually enters the fitting protocol of the effective nuclear interactions.

If we inspect the results for the surface diffuseness of the density profiles of ^{208}Pb in Table III, we see that a_n of neutrons lies in a window of 0.53 to 0.59 fm (with the majority of the models having a_n between 0.545 and 0.565 fm). The nonrelativistic interactions favor $a_n \lesssim 0.555$ fm, whereas the RMF sets favor $a_n \gtrsim 0.555$ fm. This indicates that the falloff of the neutron density of ^{208}Pb at the surface is generally faster in the interactions with a soft symmetry energy than in the interactions with a stiff symmetry energy. The surface diffuseness a_p of the proton density spans *in either* the nonrelativistic or the relativistic models almost the same window of values (0.43–0.47 fm; with the majority of the models having a_p between 0.445 and 0.465 fm). This fact is in contrast to the other 2pF parameters discussed before now. Actually, the a_p value of the proton density can be definitely larger in some nonrelativistic forces than in some relativistic forces (for example, in the case of SkM* and NL3). One finds that the total spread of a_n and a_p within the analyzed models is quite similar: about 0.05 fm in both a_n and a_p. This spread corresponds roughly to a 10% variation compared to the mean values of a_n and a_p. It is remarkable that, while among the models C_n has a significantly larger spread than C_p, the surface diffuseness a_n of the neutron density has essentially the same small spread as the surface diffuseness a_p of the proton density. As we discussed at the end of Sec. III B, this is likely imposed by the nuclear mass fits. It means that our ignorance about the neutron distribution in ^{208}Pb does not seem to produce a larger uncertainty for a_n of neutrons than for a_p of protons in the mean-field models, and that most of the uncertainty goes to the value of C_n.

The difference $C_n - C_p$ of the central radii of the nucleon densities of ^{208}Pb turns out to range approximately between 0 and 0.2 fm. It is smaller for soft symmetry energies and larger for stiff symmetry energies. We realize that the limiting situation of a halo-type distribution where the nucleon densities of ^{208}Pb have $C_n = C_p$ and $a_n > a_p$ is actually attained in the nuclear mean-field models with a very soft symmetry energy (as in HFB-8 or MSk7, where $C_n - C_p$ is even slightly negative). The difference $a_n - a_p$ of the neutron and proton surface diffuseness in ^{208}Pb comprises between nearly 0.08 and 0.1 fm in the nonrelativistic forces and between nearly 0.1 and 0.12 fm in the RMF forces. This implies that no interaction predicts $a_n - a_p$ of ^{208}Pb as close to vanishing as $C_n - C_p$ is in some forces. Thus, the limiting situation where the nucleon densities in ^{208}Pb would have $a_n = a_p$ and $C_n > C_p$ is not found in the nuclear mean-field models. Indeed, we observe in Table III that if $C_n - C_p$ becomes larger in the models, $a_n - a_p$ also tends overall to become larger. To help visualize graphically the change in the mean-field nucleon densities of ^{208}Pb from having a nearly vanishing $C_n - C_p$ or a large $C_n - C_p$, we have plotted in Fig. 3 the example of the densities of the MSk7 and NL3 interactions. On the one hand, we see that both MSk7 and NL3 models predict basically the same proton density, as expected. On the other hand, the difference between having $C_n \approx C_p$ in MSk7 and $C_n > C_p$ in NL3 can be appreciated in the higher bulk and the faster falloff at the surface of the neutron density of MSk7 compared with NL3.

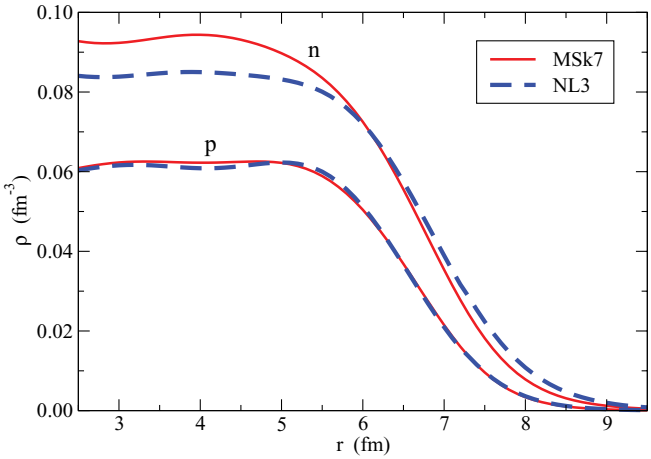

FIG. 3. (Color online) Comparison of the nucleon densities predicted in ^{208}Pb by the mean-field models MSk7 ($C_n - C_p \approx 0$ fm) and NL3 ($C_n - C_p \approx 0.2$ fm).

In summary, in ^{208}Pb the nuclear mean-field models favor the halo-type distribution with $C_n \approx C_p$ and $a_n > a_p$ if they have a very soft ("supersoft") symmetry energy. They favor a mixed-type distribution if they have mild symmetry energies. Finally, they favor a situation where C_n is clearly larger than C_p if the symmetry energy is stiff. However, we conclude that the pure skin-type distribution where $a_n - a_p = 0$ in ^{208}Pb is not supported (not even $a_n - a_p \approx 0$) by the mean-field models. Although the experimental evidence available to date on the neutron skin thickness of ^{208}Pb is compatible with the ranges of the $C_n - C_p$ and $a_n - a_p$ parameters considered in our study, it is not to be excluded that the description of a precision measurement in ^{208}Pb may require nucleon densities with $C_n - C_p$ or $a_n - a_p$ values not fitting Table III. However, a sizable deviation (such as $a_n - a_p = 0$) could mean that there is some missing physics in the isospin channel of present mean-field interactions, because once these interactions are calibrated to reproduce the observed binding energies and charge radii of nuclei they typically lead to the ranges given in Table III.

D. Application to parity-violating electron scattering

Parity-violating electron scattering is expected to be able to accurately determine the neutron density in a nucleus because the Z^0 boson couples mainly to neutrons [29,30]. Specifically, PREX [29] aims to provide a clean measurement of the neutron radius of ^{208}Pb. In this type of experiments, one measures the parity-violating asymmetry

$$A_{LR} \equiv \frac{\frac{d\sigma_+}{d\Omega} - \frac{d\sigma_-}{d\Omega}}{\frac{d\sigma_+}{d\Omega} + \frac{d\sigma_-}{d\Omega}}, \tag{15}$$

where $d\sigma_{\pm}/d\Omega$ is the elastic electron-nucleus cross section. The plus (minus) sign accounts for the fact that electrons with a positive (negative) helicity state scatter from different potentials [$V_{\pm}(r) = V_{\rm Coulomb}(r) \pm V_{\rm weak}(r)$ for ultrarelativistic electrons]. Assuming for simplicity the plane-wave Born approximation (PWBA) and neglecting nucleon form factors, the parity-violating asymmetry at momentum transfer q can be written as [30]

$$A_{LR}^{\rm PWBA} = \frac{G_F q^2}{4\pi\alpha\sqrt{2}}\left[4\sin^2\theta_W + \frac{F_n(q) - F_p(q)}{F_p(q)}\right], \quad (16)$$

where $\sin^2\theta_W \approx 0.23$ for the Weinberg angle and $F_n(q)$ and $F_p(q)$ are the form factors of the point neutron and proton densities. Because $F_p(q)$ is known from elastic electron scattering, it is clear from Eq. (16) that the largest uncertainty to compute A_{LR} comes from our lack of knowledge of the distribution of neutrons inside the nucleus. PREX intends to measure A_{LR} in ^{208}Pb with a 3% error (or smaller). This accuracy is thought to be enough to determine the neutron rms radius with a 1% error [29,30].

To compute the parity-violating asymmetry we essentially follow the procedure described in Ref. [30]. For realistic results, we perform the exact phase-shift analysis of the Dirac equation for electrons moving in the potentials $V_{\pm}(r)$ [58]. This method corresponds to the distorted-wave Born approximation (DWBA). The main inputs needed for solving this problem are the charge and weak distributions. To calculate the charge distribution, we fold the mean-field proton and neutron pointlike densities with the electromagnetic form factors provided in Ref. [59]. For the weak distribution, we fold the nucleon pointlike densities with the electric form factors reported in Ref. [30] for the coupling of Z^0 to the protons and neutrons. We neglect the strange form factor contributions to the weak density [30]. Because the experimental analysis may involve parametrized densities, in our study we use the 2pF functions extracted from the self-consistent densities of the various models. The difference between A_{LR} calculated in ^{208}Pb with the 2pF densities and with the self-consistent densities is anyway marginal at most. In Fig. 4, $A_{LR}^{\rm DWBA}$ obtained with the Fermi distributions listed in Table III is plotted against the values of $C_n - C_p$ (bottom panel) and $a_n - a_p$ (top panel). To simulate the kinematics of PREX [29], we set the electron beam energy to 1 GeV and the scattering angle to 5°, which corresponds to a momentum transfer in the laboratory frame of $q = 0.44$ fm^{-1}.

First, one can see from Fig. 4 that the mean-field calculations constrain in a rather narrow window the value of the parity-violating asymmetry in ^{208}Pb. The increasing trend of A_{LR} with decreasing $C_n - C_p$ indicates that A_{LR} is larger when the symmetry energy is softer. Note that a large value of $A_{LR} \approx 7 \times 10^{-7}$ (at 1 GeV and 5°) would be in support of a more surface than bulk origin of the neutron skin thickness of ^{208}Pb and of the halo-type density distribution for this nucleus. Second, $A_{LR}^{\rm DWBA}$ displays in good approximation a linear correlation with $C_n - C_p$ ($r = 0.978$), whereas the correlation with $a_n - a_p$ is not remarkable. Nevertheless, we found a very good description of $A_{LR}^{\rm DWBA}$ of the mean-field models—well below the 3% limit of accuracy of PREX—by

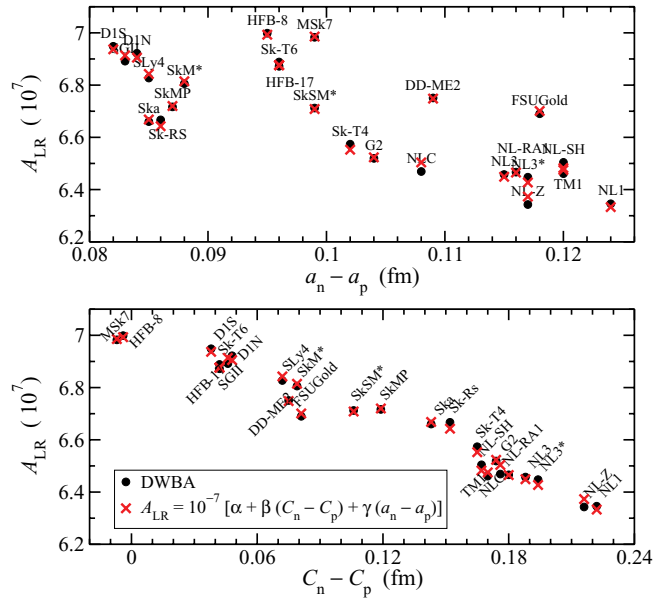

FIG. 4. (Color online) Parity-violating asymmetry for 1 GeV electrons at 5° scattering angle calculated from the 2pF neutron and proton density distributions of ^{208}Pb in nuclear mean-field models.

means of a fit in $C_n - C_p$ and $a_n - a_p$ [(red) crosses in Fig. 4]:

$$A_{LR}^{\rm fit} = [\alpha + \beta(C_n - C_p) + \gamma(a_n - a_p)] \times 10^{-7}, \quad (17)$$

with $\alpha = 7.33$, $\beta = -2.45$ fm^{-1}, and $\gamma = -3.62$ fm^{-1}.

Parametrization (17) may be easily understood if we consider the PWBA expression of A_{LR} given in Eq. (16). At low momentum transfer, the form factors $F_n(q)$ and $F_p(q)$ of the neutron and proton densities (these are point densities in PWBA) can be expanded to first order in q^2, so the numerator inside brackets in Eq. (16) becomes $-(q^2/6)\,(\langle r^2\rangle_n - \langle r^2\rangle_p)$. In 2pF density distributions, we have $\langle r^2\rangle_q = (3/5)C_q^2 + (7\pi^2/5)a_q^2$. Now, assuming constancy of $F_p(q^2)$ in the nuclear models and taking into account that $C_n + C_p \gg C_n - C_p$ and $a_n + a_p \gg a_n - a_p$, it is reasonable to assume that the variation of A_{LR} is dominated by the change of $C_n - C_p$ and $a_n - a_p$ as proposed in Eq. (17).

In the analysis of a measurement of A_{LR} in ^{208}Pb through parametrized Fermi densities, one could set C_p and a_p to those known from experiment [40] and then vary C_n and a_n in Eq. (17) to match the measured value. According to the predictions of the models in Table III, it would be reasonable to restrict this search to windows of about 0–0.22 fm for $C_n - C_p$ and 0.08–0.125 fm for $a_n - a_p$. Therefore, the result of a measurement of the parity-violating asymmetry together with Eq. (17) (or Fig. 4) would allow not only estimation of the neutron rms radius of ^{208}Pb but would also allow us to obtain some insight about the neutron density profile in this nucleus. This assumes that the experimental value for A_{LR} will fall in, or at least will be not far from, the region allowed by the mean-field calculations at the same kinematics.

IV. SUMMARY

We investigated using Skyrme, Gogny, and relativistic mean-field models of nuclear structure whether the difference between the peripheral neutron and proton densities that gives rise to the neutron skin thickness of ^{208}Pb is because of an enlarged bulk radius of neutrons with respect to that of protons or, rather, because of the difference between the widths of the neutron and proton surfaces. The decomposition of the neutron skin thickness in bulk and surface components was obtained through two-parameter Fermi distributions fitted to the self-consistent nucleon densities of the models.

Nuclear models that correspond to a soft symmetry energy, like various nonrelativistic mean-field models, favor the situation where the size of the neutron skin thickness of ^{208}Pb is divided similarly into bulk and surface components. If the symmetry energy of the model is "supersoft", the surface part even becomes dominant. Instead, nuclear models that correspond to a stiff symmetry energy, like most of the relativistic models, predict a bulk component about twice as large as the surface component. We have found that the size of the surface component changes little among the various nuclear mean-field models and that the known linear correlation of Δr_{np} of ^{208}Pb with the density derivative of the nuclear symmetry energy arises from the bulk part of Δr_{np}. The latter result implies that an experimental determination of the equivalent sharp radius of the neutron density of ^{208}Pb could be as useful for the purpose of constraining the density-dependent nuclear symmetry energy as a determination of the neutron rms radius.

We discussed the shapes of the 2pF distributions predicted for ^{208}Pb by the nuclear mean-field models in terms of the so-called halo-type ($C_n - C_p = 0$) and skin-type ($a_n - a_p = 0$) distributions of frequent use in experiment. It turns out that the theoretical models can accommodate the halo-type distribution in ^{208}Pb if the symmetry energy is supersoft. However, they do no support a purely skin-type distribution in this nucleus, even if the model has a largely stiff symmetry energy. Let us mention that the information on neutron densities from antiprotonic atoms favored the halo-type over the skin-type distribution [35,36].

We closed our study with a calculation of the asymmetry A_{LR} for parity-violating electron scattering off ^{208}Pb in conditions as in the recently run ^{208}Pb parity radius experiment [29], using the equivalent 2pF shapes of the models. This allowed us to find a simple parametrization of A_{LR} in terms of the differences $C_n - C_p$ and $a_n - a_p$ of the parameters of the nucleon distributions. With a measured value of the parity-violating asymmetry, it would provide a new correlation between the central radius and the surface diffuseness of the distribution of neutrons in ^{208}Pb, assuming the same properties of the proton density known from experiment.

ACKNOWLEDGMENTS

Work was partially supported by the Spanish Consolider-Ingenio 2010 Programme CPAN CSD2007-00042 and by Grants No. FIS2008-01661 from MICIN (Spain) and FEDER, No. 2009SGR-1289 from Generalitat de Catalunya (Spain), and No. N202 231137 from MNiSW (Poland).

[1] G. Fricke, C. Bernhardt, K. Heilig, L. A. Schaller, L. Schellenberg, E. B. Shera, and C. W. de Jager, At. Data Nucl. Data Tables **60**, 177 (1995).
[2] B. A. Brown, Phys. Rev. Lett. **85**, 5296 (2000).
[3] S. Typel and B. A. Brown, Phys. Rev. C **64**, 027302 (2001).
[4] M. Centelles, M. Del Estal, X. Viñas, and S. K. Patra, in *The Nuclear Many-Body Problem 2001*, edited by W. Nazarewicz and D. Vretenar, NATO Advanced Studies Institute Series B: Physics, Vol. 53 (Kluwer, Dordrecht, 2002), p. 97.
[5] R. J. Furnstahl, Nucl. Phys. A **706**, 85 (2002).
[6] P. Danielewicz, Nucl. Phys. A **727**, 233 (2003).
[7] M. Baldo, C. Maieron, P. Schuck, and X. Viñas, Nucl. Phys. A **736**, 241 (2004).
[8] S. S. Avancini, J. R. Marinelli, D. P. Menezes, M. M. W. Moraes, and C. Providência, Phys. Rev. C **75**, 055805 (2007).
[9] M. Centelles, X. Roca-Maza, X. Viñas, and M. Warda, Phys. Rev. Lett. **102**, 122502 (2009).
[10] M. Warda, X. Viñas, X. Roca-Maza, and M. Centelles, Phys. Rev. C **80**, 024316 (2009).
[11] I. Vidaña, C. Providência, A. Polls, and A. Rios, Phys. Rev. C **80**, 045806 (2009).
[12] W. D. Myers and W. J. Świątecki, Ann. Phys. (NY) **55**, 395 (1969); **84**, 186 (1974).
[13] W. D. Myers and W. J. Świątecki, Nucl. Phys. A **336**, 267 (1980).
[14] C. J. Horowitz and J. Piekarewicz, Phys. Rev. Lett. **86**, 5647 (2001); Phys. Rev. C **64**, 062802 (2001).
[15] A. E. L. Dieperink, Y. Dewulf, D. Van Neck, M. Waroquier, and V. Rodin, Phys. Rev. C **68**, 064307 (2003).
[16] T. Sil, M. Centelles, X. Viñas, and J. Piekarewicz, Phys. Rev. C **71**, 045502 (2005).
[17] A. W. Steiner, M. Prakash, J. M. Lattimer, and P. J. Ellis, Phys. Rep. **411**, 325 (2005).
[18] J. M. Lattimer and M. Prakash, Phys. Rep. **442**, 109 (2007).
[19] S. K. Dhiman, R. Kumar, and B. K. Agrawal, Phys. Rev. C **76**, 045801 (2007).
[20] S. K. Samaddar, J. N. De, X. Viñas, and M. Centelles, Phys. Rev. C **76**, 041602(R) (2007).
[21] A. Klimkiewicz *et al.*, Phys. Rev. C **76**, 051603(R) (2007).
[22] B. A. Li, L. W. Chen, and C. M. Ko, Phys. Rep. **464**, 113 (2008).
[23] J. Xu, L. W. Chen, B. A. Li, and H. R. Ma, Astrophys. J. **697**, 1549 (2009).
[24] H. S. Than, D. T. Khoa, and N. V. Giai, Phys. Rev. C **80**, 064312 (2009).
[25] X. Y. Sun, D. Q. Fang, Y. G. Ma, X. Z. Cai, J. G. Chen, W. Guo, W. D. Tian, and H. W. Wang, Phys. Lett. B **682**, 396 (2010).
[26] M. Centelles, S. K. Patra, X. Roca-Maza, B. K. Sharma, P. D. Stevenson, and X. Viñas, J. Phys. G **37**, 075107 (2010).
[27] A. Carbone, G. Colò, A. Bracco, L. G. Cao, P. F. Bortignon, F. Camera, and O. Wieland, Phys. Rev. C **81**, 041301(R) (2010).
[28] L. W. Chen, C. M. Ko, B. A. Li, and J. Xu, Phys. Rev. C **82**, 024321 (2010).
[29] K. Kumar, P. A. Souder, R. Michaels, and G. M. Urciuoli, spokespersons [http://hallaweb.jlab.org/parity/prex].

[30] C. J. Horowitz, S. J. Pollock, P. A. Souder, and R. Michaels, Phys. Rev. C **63**, 025501 (2001).
[31] S. Karataglidis, K. Amos, B. A. Brown, and P. K. Deb, Phys. Rev. C **65**, 044306 (2002).
[32] B. C. Clark, L. J. Kerr, and S. Hama, Phys. Rev. C **67**, 054605 (2003).
[33] A. Krasznahorkay *et al.*, Phys. Rev. Lett. **82**, 3216 (1999).
[34] A. Krasznahorkay *et al.*, Nucl. Phys. A **731**, 224 (2004).
[35] A. Trzcińska, J. Jastrzębski, P. Lubiński, F. J. Hartmann, R. Schmidt, T. von Egidy, and B. Kłos, Phys. Rev. Lett. **87**, 082501 (2001).
[36] J. Jastrzębski, A. Trzcińska, P. Lubiński, B. Kłos, F. J. Hartmann, T. von Egidy, and S. Wycech, Int. J. Mod. Phys. E **13**, 343 (2004).
[37] E. Friedman and A. Gal, Nucl. Phys. A **724**, 143 (2003).
[38] E. Friedman, A. Gal, and J. Mareš, Nucl. Phys. A **761**, 283 (2005); E. Friedman, Hyperfine Interact. **193**, 33 (2009).
[39] T. Dong, Y. Chu, Z. Ren, and Z. Wang, Phys. Rev. C **79**, 014317 (2009).
[40] M. Warda, X. Viñas, X. Roca-Maza, and M. Centelles, Phys. Rev. C **81**, 054309 (2010).
[41] R. W. Hasse and W. D. Myers, *Geometrical Relationships of Macroscopic Nuclear Physics* (Springer-Verlag, Heidelberg, 1988).
[42] S. Goriely, N. Chamel, and J. M. Pearson, Phys. Rev. Lett. **102**, 152503 (2009).
[43] F. Chappert, M. Girod, and S. Hilaire, Phys. Lett. B **668**, 420 (2008).
[44] S. K. Patra, M. Centelles, X. Viñas, and M. Del Estal, Phys. Rev. C **65**, 044304 (2002).
[45] A. Sulaksono, T. Mart, T. J. Bürvenich, and J. A. Maruhn, Phys. Rev. C **76**, 041301(R) (2007).
[46] B. G. Todd-Rutel and J. Piekarewicz, Phys. Rev. Lett. **95**, 122501 (2005).
[47] G. A. Lalazissis, T. Nikšić, D. Vretenar, and P. Ring, Phys. Rev. C **71**, 024312 (2005).
[48] G. A. Lalazissis, S. Karatzikos, R. Fossion, D. Pena Arteaga, A. V. Afanasjev, and P. Ring, Phys. Lett. B **671**, 36 (2009).
[49] S. Goriely, N. Chamel, and J. M. Pearson, Phys. Rev. C **82**, 035804 (2010).
[50] B. G. Todd and J. Piekarewicz, Phys. Rev. C **67**, 044317 (2003).
[51] J. Piekarewicz and M. Centelles, Phys. Rev. C **79**, 054311 (2009).
[52] B. Kłos *et al.*, Phys. Rev. C **76**, 014311 (2007).
[53] B. A. Brown, G. Shen, G. C. Hillhouse, J. Meng, and A. Trzcińska, Phys. Rev. C **76**, 034305 (2007).
[54] L. W. Chen, C. M. Ko, and B. A. Li, Phys. Rev. C **72**, 064309 (2005).
[55] A. W. Steiner and B. A. Li, Phys. Rev. C **72**, 041601(R) (2005).
[56] J. Zenihiro *et al.*, Phys. Rev. C **82**, 044611 (2010).
[57] D. H. Wen, B. A. Li, and L. W. Chen, Phys. Rev. Lett. **103**, 221102 (2009).
[58] X. Roca-Maza, M. Centelles, F. Salvat, and X. Viñas, Phys. Rev. C **78**, 044332 (2008).
[59] J. Friedrich and T. Walcher, Eur. Phys. J. A **17**, 607 (2003).